

# Modeling and Simulation for UAV Air-to-Ground mmWave Channels

Lele Cheng<sup>1</sup>, Qiuming Zhu<sup>1,\*</sup>, Cheng-Xiang Wang<sup>2,3,\*</sup>, Weizhi Zhong<sup>1</sup>, Boyu Hua<sup>1</sup>, Shan Jiang<sup>1</sup>

<sup>1</sup>The Key Laboratory of Dynamic Cognitive System of Electromagnetic Spectrum Space,

College of Electronic and Information Engineering,

Nanjing University of Aeronautics and Astronautics, Nanjing 211106, China

<sup>2</sup>National Mobile Communications Research Laboratory, School of Information Science and Engineering,

Southeast University, Nanjing 210096, China

<sup>3</sup>Purple Mountain Laboratories, Nanjing 211111, China

\*Corresponding author

Email: {cxl\_2017, zhuqiuming}@nuaa.edu.cn, chxwang@seu.edu.cn, {zhongwz,byhua}@nuaa.edu.cn

**Abstract**—In this paper, we propose a new three-dimensional (3D) channel model for the millimeter wave (mmWave) communication links between the Unmanned Aerial Vehicle (UAV) and vehicle. The new model applies the ray tracing (RT) theory in traditional geometry-based stochastic model (GBSM), and it also takes the specific features of mmWave propagation into account. Meanwhile, the time evolving algorithms of channel parameters, i.e., communication distance, propagation angles, path delays, and powers are analyzed and illustrated. On these basis, the mmWave channel simulations at 28 GHz are conducted under the campus scenario. Simulation results demonstrate that the proposed model can generate the non-stationary Air-to-Ground mmWave channels, of which statistical properties have a good agreement with the measured ones. Therefore, this model is valuable for the system design, performance optimization, and evaluation of UAV mmWave communication systems.

**Index Terms**—mmWave channel, channel model, UAV, air-to-ground (A2G) channel, statistical properties.

## I. INTRODUCTION

The wireless communication systems based on UAVs have found a wide range of applications due to its low cost, simple operation, flexible configuration, and portability [1]. Recent studies have also suggested the usage of mmWave band to satisfy the increased bandwidth demand and transmission rate for UAV communications [2]–[5]. Thus, the UAV-assisted mmWave communication has become a hot research topic [6]–[8]. Most of literatures focused on the techniques in UAV mmWave communication systems and the benefits they can bring, but the propagation channel statistical characteristics are less mentioned [9], [10]. However, a deep understanding of UAV mmWave channels is vital for the system design and performance optimization.

Recently, the authors in [11] proposed a 3D mmWave channel model, which was described as a function of the UAV movement and channel gain. By taking the line-of-sight (LoS) blockage into account, a mmWave path loss model considering the LoS congestion caused by human body was established to optimize the deployment of UAV-assisted station in [12]. Considering the smooth power transition of birth-death non-line-of-sight (NLoS) paths, the authors in [13] proposed a

new 3D non-stationary UAV multiple-input multiple-output (MIMO) channel model, and the statistical properties were also derived. Furthermore, taking the 3D antenna arrays and 3D arbitrary trajectories of the UAV and mobile terminal into account, the authors in [14] proposed a GBSM for UAV mmWave channels which included the LoS, ground reflection, and other single-bounce (SB) components, and the theoretical statistical properties and the angular distribution were also analyzed. Meanwhile, several measurement campaigns and the RT method for UAV channels were found in [15]–[18]. By the software simulation method, the authors in [15] studied the characteristics of UAV mmWave channels at different flight altitudes in cities, suburbs, farms, and over the sea as well. Then, the space-time characteristics of UAV mmWave channels under different altitudes and scenarios were analyzed in [16]. An application scenario combining the RT method and channel emulation in multi-probe anechoic chamber for UAV A2G connections was demonstrated in [17], and the channel properties, i.e., the power delay profile and delay spread were emulated. The results of UAV channel measurements in suburban environments were presented in [18], which provided models of path loss, delay spread and the number of multipath components.

Notably, the time resolution in mmWave communication systems is much higher than that in traditional radio systems. For mmWave propagation channels, the geometric optical transmission characteristics are highlighted, therefore it is suitable to use the RT method to analyze and model the channel. However, this method is usually used in the static scenarios and cannot be used to model the dynamic mmWave channel directly. This paper aims to fill the above research gaps. In this paper, a 3D geometric channel model for UAV mmWave communications is proposed. The new model combines the RT principle and GBSM framework, and takes into account the space-time characteristics of UAV flight. In addition, the calculation methods of geometric parameters and channel parameters are analyzed and derived.

The remainder of this paper is organized as follows. In Section II, a 3D UAV mmWave channel model based on the

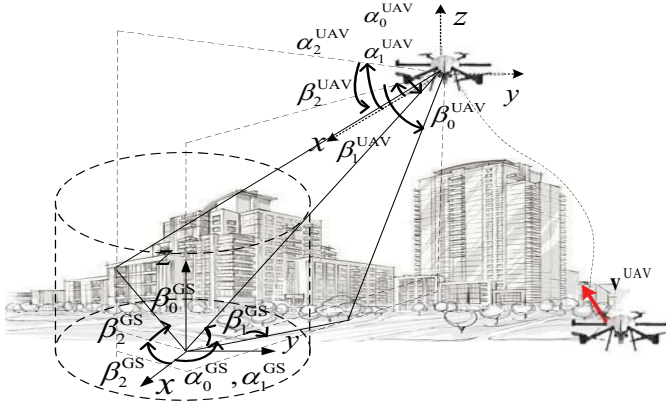


Fig. 1. The UAV-assisted mmWave communication channel.

RT theory and GBSM framework is proposed. The computation methods of channel parameters as well as the statistical analysis of channel parameters are presented in Section III. Simulation and validation results are analyzed in Section IV. Finally, conclusions are given in Section V.

## II. UAV MMWAVE CHANNEL MODEL

A typical A2G communication system, which includes a downlink communication channel between the UAV and GS with a 3D arbitrary moving trajectory, is shown in Fig. 1. The authors in [19] have proven that the channel between the UAV and GS includes multiple path components such as the LoS component and several NLoS components caused by the surrounding scatterers. The azimuth angle of departure (AAoD)  $\alpha_l^{\text{UAV}}$ , elevation angle of departure (EAoD)  $\beta_l^{\text{UAV}}$ , azimuth angle of arrival (AAoA)  $\alpha_l^{\text{GS}}$ , and elevation angle of arrival (EAoA)  $\beta_l^{\text{GS}}$  are time-variant and related with the particular locations of transmitter, receiver, and scattering buildings.

Considering the dynamic A2G propagation scenario, both the delay dispersion and the angular dispersion play an important role. In a stochastic description way, it's assumed that the channel, which includes a LoS component and several NLoS components, which can be expressed by the sum of rays with different delays, amplitudes, and two-dimensional angles as

$$h(t, \tau, \alpha, \beta) = \sum_{l=0}^{L(t)} P_l(t) e^{\frac{2\pi}{\lambda_0} \int_0^t (\mathbf{v}^{\text{UAV}})^T \mathbf{r}_l^{\text{GS}}(t) dt + \psi_l} \cdot \delta(t - \tau_l(t)) \delta(\alpha^{\text{UAV}} - \alpha_l^{\text{UAV}}(t)) \cdot (\beta^{\text{UAV}} - \beta_l^{\text{UAV}}(t)) \delta(\alpha^{\text{GS}} - \alpha_l^{\text{GS}}(t)) \cdot \delta(\beta^{\text{GS}} - \beta_l^{\text{GS}}(t)) \quad (1)$$

$$\beta_0^{\text{GS/UAV}}(t) = \arctan\left(\frac{\mathbf{L}_{l,z}^{\text{UAV/GS}}(t) - \mathbf{L}_{l,z}^{\text{GS/UAV}}(t)}{\sqrt{(\mathbf{L}_{l,x}^{\text{UAV/GS}}(t) - \mathbf{L}_{l,x}^{\text{GS/UAV}}(t))^2 + (\mathbf{L}_{l,y}^{\text{UAV/GS}}(t) - \mathbf{L}_{l,y}^{\text{GS/UAV}}(t))^2}}\right) \quad (8)$$

$$\alpha_0^{\text{GS/UAV}}(t) = \arcsin\left(\frac{\mathbf{L}_{l,y}^{\text{UAV/GS}}(t) - \mathbf{L}_{l,y}^{\text{GS/UAV}}(t)}{\sqrt{(\mathbf{L}_{l,x}^{\text{UAV/GS}}(t) - \mathbf{L}_{l,x}^{\text{GS/UAV}}(t))^2 + (\mathbf{L}_{l,y}^{\text{UAV/GS}}(t) - \mathbf{L}_{l,y}^{\text{GS/UAV}}(t))^2}}\right) \quad (9)$$

where  $P_l(t)$ ,  $\psi_l$ , and  $\tau_l(t)$  denote the power gain, random phase, and time delay of  $l$ th propagation path, respectively,  $L(t)$  denotes the number of valid signal rays, and  $\lambda_0$  denotes the wavelength. In (1),  $\mathbf{v}^{\text{UAV}}$  means the velocity of UAV, and it can be expressed as

$$\mathbf{v}^{\text{UAV}} = v^{\text{UAV}} \begin{bmatrix} \cos \beta_v \cos \alpha_v \\ \cos \beta_v \sin \alpha_v \\ \sin \beta_v \end{bmatrix} \quad (2)$$

where  $\alpha_v$  and  $\beta_v$  represent the azimuth and elevation angles of UAV velocity, respectively. Similarly, the normalized direction vectors of the receiving and transmitting signals within the  $l$ th propagation path  $\mathbf{r}_l^{\text{GS/UAV}}(t)$  can be expressed by  $\alpha_l^{\text{UAV}}$ ,  $\beta_l^{\text{UAV}}$ ,  $\alpha_l^{\text{GS}}$ , and  $\beta_l^{\text{GS}}$  as

$$\mathbf{r}_l^{\text{GS/UAV}}(t) = \begin{bmatrix} \cos \beta_l^{\text{GS/UAV}}(t) \cos \alpha_l^{\text{GS/UAV}}(t) \\ \cos \beta_l^{\text{GS/UAV}}(t) \sin \alpha_l^{\text{GS/UAV}}(t) \\ \sin \beta_l^{\text{GS/UAV}}(t) \end{bmatrix}. \quad (3)$$

## III. COMPUTATION AND STATISTICAL ANALYSIS OF CHANNEL PARAMETERS

### A. Geometry-based Channel Parameters

#### 1) Angle parameters

In the proposed model, the propagation angles are time-variant and related with the particular locations of transmitter, receiver, and scatterers, and they can be calculated in a deterministic way. Firstly, let us set  $\mathbf{L}_{l,x}^{\text{UAV/GS/S}}$ ,  $\mathbf{L}_{l,y}^{\text{UAV/GS/S}}$ , and  $\mathbf{L}_{l,z}^{\text{UAV/GS/S}}$  as the  $x$ ,  $y$ , and  $z$  components of corresponding 3D locations. Then, by using the transform from the Cartesian coordination to the spherical coordination. The time-variant EAoD, EAoA and AAoD, AAoA within the  $n$ th NLoS path can be calculated by

$$\beta_l^{\text{UAV}}(t) = \arctan\left(\frac{\mathbf{L}_{l,z}^{\text{S}} - \mathbf{L}_{l,z}^{\text{UAV}}(t)}{\sqrt{(\mathbf{L}_{l,x}^{\text{S}} - \mathbf{L}_{l,x}^{\text{UAV}}(t))^2 + (\mathbf{L}_{l,y}^{\text{S}} - \mathbf{L}_{l,y}^{\text{UAV}}(t))^2}}\right) \quad (4)$$

$$\alpha_l^{\text{UAV}}(t) = \arcsin\left(\frac{\mathbf{L}_{l,y}^{\text{S}} - \mathbf{L}_{l,y}^{\text{UAV}}(t)}{\sqrt{(\mathbf{L}_{l,x}^{\text{S}} - \mathbf{L}_{l,x}^{\text{UAV}}(t))^2 + (\mathbf{L}_{l,y}^{\text{S}} - \mathbf{L}_{l,y}^{\text{UAV}}(t))^2}}\right) \quad (5)$$

$$\beta_l^{\text{GS}} = \arctan\left(\frac{\mathbf{L}_{l,z}^{\text{S}} - \mathbf{L}_{l,z}^{\text{GS}}}{\sqrt{(\mathbf{L}_{l,x}^{\text{S}} - \mathbf{L}_{l,x}^{\text{GS}})^2 + (\mathbf{L}_{l,y}^{\text{S}} - \mathbf{L}_{l,y}^{\text{GS}})^2}}\right) \quad (6)$$

$$\alpha_l^{\text{GS}} = \arcsin\left(\frac{\mathbf{L}_{l,y}^{\text{S}} - \mathbf{L}_{l,y}^{\text{GS}}}{\sqrt{(\mathbf{L}_{l,x}^{\text{S}} - \mathbf{L}_{l,x}^{\text{GS}})^2 + (\mathbf{L}_{l,y}^{\text{S}} - \mathbf{L}_{l,y}^{\text{GS}})^2}}\right). \quad (7)$$

Similarly, the mean values of time-variant EAoD, EAoA and AAoD, AAoA for the LoS path can be calculated by (8)–(9).

### 2) Delay parameters

In order to calculate the delay parameters, the propagation distance is needed. Due to the movement of UAV, the distance between the UAV and GS changes over time. In reality, the initial locations can be obtained by a measurement campaign, user definition, or random generation. The 3D location vectors  $\mathbf{L}^{\text{UAV}}(t)$ ,  $\mathbf{L}_l^{\text{S}}$  of the UAV and the  $l$ th scatterer at the time instant  $t$  can be calculated by

$$\begin{aligned}\mathbf{L}_l^{\text{S}} &= D_l^{\text{GS,S}} \cdot \mathbf{r}_l^{\text{GS}} \\ \mathbf{L}^{\text{UAV}}(t_0) &= D^{\text{UAV}}(t_0) \cdot \mathbf{r}_0^{\text{GS}}(t_0) \\ \mathbf{L}^{\text{UAV}}(t) &= \mathbf{L}^{\text{UAV}}(t - \Delta t) + \mathbf{v}^{\text{UAV}} \cdot \Delta t\end{aligned}\quad (10)$$

where  $D_l^{\text{GS,S}}$  and  $D^{\text{UAV}}(t_0)$  denote the distances between the GS and  $S_l$ , and the initial distance between the GS and UAV. Thus, based on the time-variant location of UAV, the corresponding distances between GS and UAV, scatterer and UAV can be calculated by following iterative algorithms, respectively, as

$$\begin{aligned}D^{\text{UAV}}(t + \Delta t) &= \|\mathbf{L}^{\text{UAV}}(t + \Delta t)\| \\ &= \sqrt{D^{\text{UAV}}(t)^2 + (\|\mathbf{v}^{\text{UAV}}\| \Delta t)^2 + 2D^{\text{UAV}}(t)\|\mathbf{v}^{\text{UAV}}\|\Delta t \cdot \left( \begin{aligned} &\cos \beta_0^{\text{GS}}(t) \cos \alpha_v(t) \cos(\alpha_0^{\text{GS}}(t) - \beta_v(t)) \\ &+ \sin \beta_0^{\text{GS}}(t) \sin \beta_v(t) \end{aligned} \right)}\end{aligned}\quad (11)$$

$$\begin{aligned}D_l^{\text{S,UAV}}(t + \Delta t) &= \|\mathbf{L}^{\text{UAV}}(t + \Delta t) - \mathbf{L}_l^{\text{S}}\| \\ &= \sqrt{\left( D^{\text{UAV}}(t) - D_l^{\text{GS}} \right)^2 + (\|\mathbf{v}^{\text{UAV}}\| \Delta t)^2 + 2 \left( D^{\text{UAV}}(t) - D_l^{\text{GS}} \right) \|\mathbf{v}^{\text{UAV}}\| \Delta t \cdot \left( \begin{aligned} &\cos \beta_l^{\text{GS}}(t) \cos \alpha_v(t) \cos(\alpha_l^{\text{GS}}(t) - \beta_v(t)) \\ &+ \sin \beta_l^{\text{GS}}(t) \sin \beta_v(t) \end{aligned} \right)}\end{aligned}\quad (12)$$

The time-variant delay of the  $l$ th NLoS path at time  $t$  can be expressed as

$$\tau_l(t) = \frac{\left( D_l^{\text{GS,S}} + D_l^{\text{S,UAV}}(t) \right)}{c}\quad (13)$$

where,  $c$  represents the speed of light. Similarly, the time-variant delay of LoS path can be calculated as

$$\tau_0(t) = \frac{D^{\text{UAV}}(t)}{c}\quad (14)$$

### 3) Power gain parameters

The propagation condition of LoS path in the UAV-to-ground communications is similar to the free space environment. In this paper, the time-variant power gain of LoS path in our model can be calculated by

$$\begin{aligned}P_0(t) &= 10 \log \frac{P^{\text{UAV}}}{P^{\text{GS}}(t)} \\ &= 32.44 + 20 \log(f) + 20 \log(D^{\text{UAV}}(t))\end{aligned}\quad (15)$$

where  $P^{\text{UAV}}$  and  $P^{\text{GS}}(t)$  are the transmitted and received signal power, respectively,  $f$  denotes the carrier frequency in MHz.

In addition, the power gains of reflection and scattering paths can be obtained by adding a certain extra loss to the above reference value as

$$P_l(t) = P_0(t) + L_l(t)\quad (16)$$

where  $L_l(t) = -10 \log |R_F e^{-j\Delta\varphi(t)}|^2$  is an additional loss,  $R_F$  is the reflection coefficient,  $\Delta\varphi(t)$  is the phase difference between the reflection path and direct path, and it can be calculated by

$$\Delta\varphi(t) = \frac{2\pi}{\lambda} \Delta r(t)\quad (17)$$

where  $\Delta r(t)$  denotes the distance difference between the reflection path and direct path, and it can be expressed as

$$\Delta r(t) = D_l^{\text{GS,S}} + D_l^{\text{S,UAV}}(t) - D^{\text{UAV}}(t).\quad (18)$$

### B. Statistical Properties of Channel Parameters

In this section, the statistical properties of channel parameters is obtained by RT method under the campus scenario, which would be used to reproduce the UAV mmWave channel in the next section. For the campus scenario of Nanjing University of Aeronautics and Astronautics (NUAA), we find that the main area contains 66 buildings with an average height of about 30 m. The surface of buildings is concrete, and the open ground of campus is mostly wet soil. Before we run the RT method, in order to reduce the computation complexity, the digital map is simplified by using the existing two-dimensional building data combined with the measured building height. Fig. 2 shows the scenario RT needed based on the satellite view of NUAA Campus and five flight trajectories of UAV.

We set the mmWave frequency of UAV-to-ground communication 28 GHz and the bandwidth is 500 M. The UAV and vehicle are all equipped with vertically polarized omnidirectional antennas. The height of vehicle antenna is 2 m, the flight height of UAV is 75 m, and the flight speed is 10 m/s. The whole simulation time is 120 seconds and 120 measurement points are selected. Note that the propagation characteristic of mmWave communications strongly depends on the UAV trajectories. In order to obtain the universal

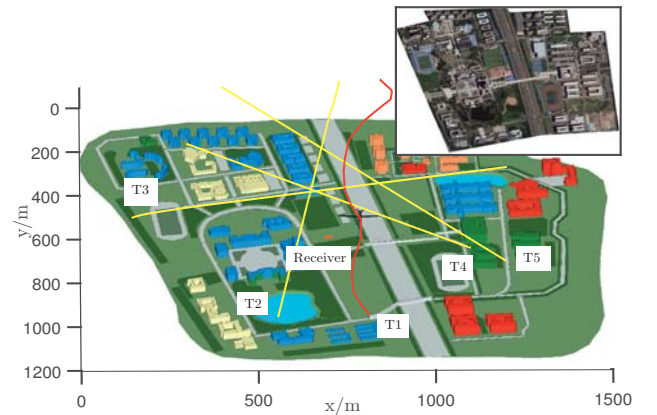


Fig. 2. The RT scenario and satellite view of NUAA Campus.

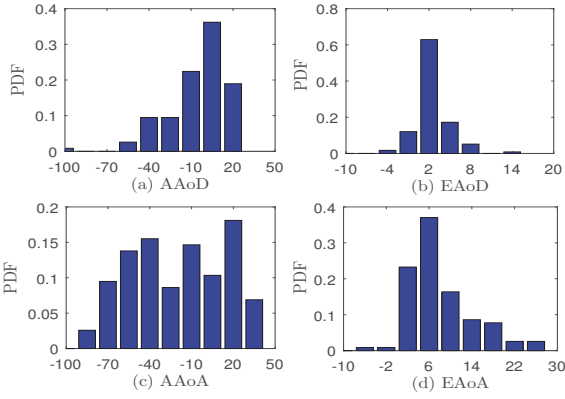


Fig. 3. Statistical distributions of angles.

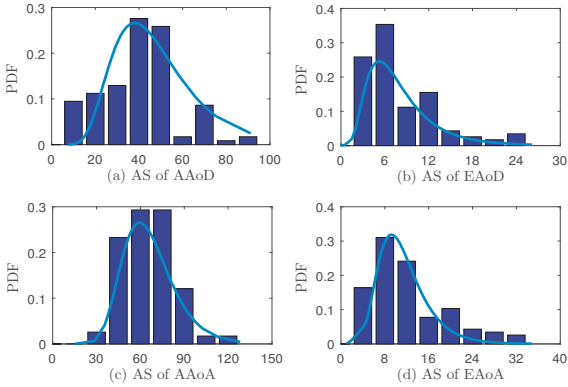


Fig. 4. Statistical distributions of ASs.

statistical properties, we select five typical trajectories which always have a LoS path to analyze.

### 1) Angle parameters

Statistical distributions of AAoD, AAoA and EAoD, EAoA are shown in Fig. 3. It should be mentioned that these results are close to the measured ones in [20] and [21]. Furthermore, the statistical distribution of angle spread (AS) is also given in Fig. 4, which shows that the lognormal distribution can fit the data very well. The average values of AS of AAoD, EAoD, AAoA, and EAoA are  $40.81^\circ$ ,  $8.07^\circ$ ,  $66.31^\circ$ , and  $12.30^\circ$ , respectively. The parameters of lognormal distribution  $\mu$  of AS of AAoD, EAoD, AAoA, and EAoA are 3.58, 1.94, 4.16, and 2.37, respectively, and  $\sigma$  of AS of AAoD, EAoD, AAoA, and EAoA are 0.52, 0.54, 0.27, and 0.52, respectively.

### 2) Delay parameters

The distribution of path delay are shown in Fig. 5(a). The delay spread in Fig. 5(b) represents the power-weighted root mean square value of the path delay. It shows that the path delay of ground reflection path is 100-200 ns, and coexists with the LoS path for most of time, which is also the main factor affecting the performance of the receiver. The delay spread ranges from 0 ns to 700 ns and mainly concentrates between 40 ns and 60 ns, which consistent with the result in the literature [22].

### 3) Power gain parameters

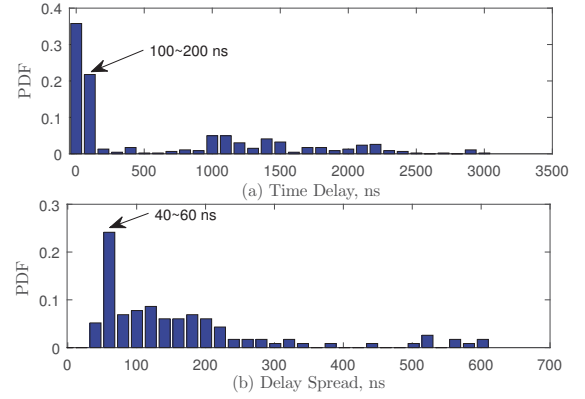


Fig. 5. Statistical distributions of path delay and DS.

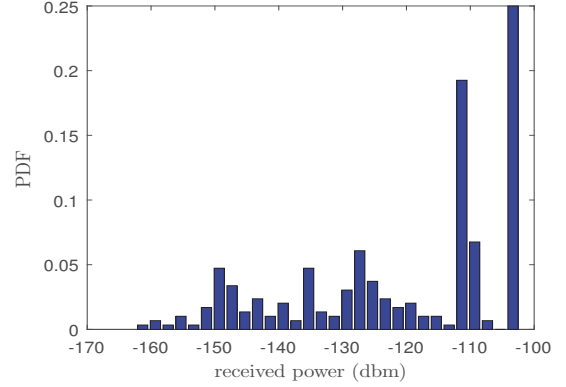


Fig. 6. Statistical distribution of power.

To obtain the power gain distribution, we fix the UAV to fly around the vehicle with the same distance such as 150 m. Fig. 6 illustrates the statistical distributions of power gain. As we can see from the figure, the power of LoS path always exists and it is the main component of total power, and the received power is mostly concentrated between -110 dbm and -100 dbm, due to the always existing direct path. The ground reflect path exists at most of time, but the other NLoS path only exist for a short time and the power of NLoS path varies with scattering environment, which leads to the fragmented distribution of power between -160 dbm and -120 dbm.

## IV. UAV MMWAVE CHANNEL SIMULATION

Based on the above calculation methods and statistical results of UAV mmWave channel parameters, we ran the proposed model to reproduce the mmWave channel in a stochastic way. The instantaneous normalized probability density functions of AoAs and AoDs at different time instants during the flight are given in Fig. 7(a) and Fig. 7(b), and they can be obtained from the statistical distribution of AS and angular mean as given in Fig. 3 and Fig. 4. As we can see that both the AoA and AoD are time-variant, and the change of departure angle is greater than the that of arrival angle. The output CIR are given in Fig. 8. It clearly shows the appearance and disappearance of each NLoS path and the time-variant path delay during the flight. The rapid movement of UAV results in the random birth

and death of scattering clusters, which are also consistent with the statistical analyzed results in Section III.

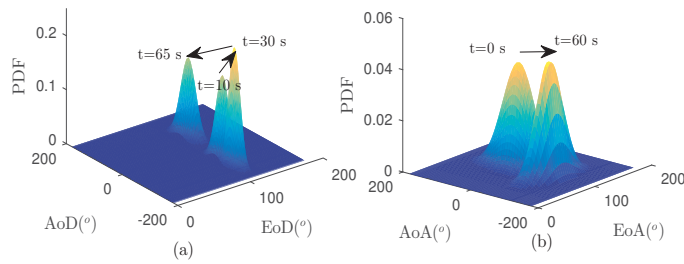


Fig. 7. Statistical distributions of (a) Angle of departure and (b) Angle of arrival.

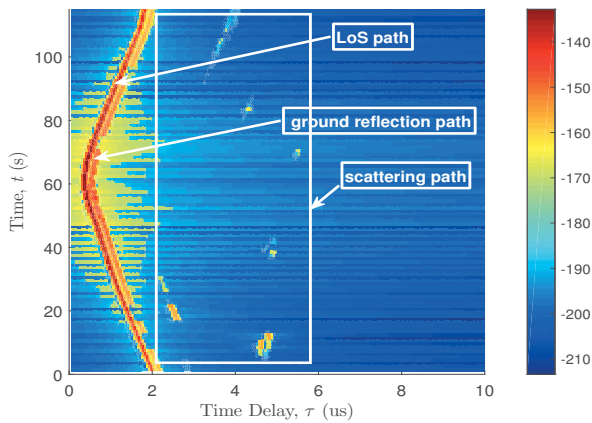


Fig. 8. Time-variant channel impulse response.

## V. CONCLUSIONS

In this paper, a geometry-based non-stationary channel model for 3D UAV mmWave communications has been proposed. The iteration calculation method of time-varying geometric parameters and channel parameters have been derived. Based on the statistical results of channel parameters obtained by the RT method, the angle evolution characteristics and CIR have been reproduced. The simulation results have shown that the reconstructed channel is consistent with the theoretical one. The proposed model and simulation method can be used to evaluate the performance of UAV mmWave communication systems, and provide theoretical basis for optimizing the UAV system design, air base station layout and cruise routes.

## ACKNOWLEDGMENT

This work was supported by the National Key R&D Program of China (No. 2018YFB1801101), the National Key Scientific Instrument and Equipment Development Project (No. 61827801), the National Natural Science Foundation of China (No. 61960206006), the Research Fund of National Mobile Communications Research Laboratory, Southeast University (No. 2020B01), the Fundamental Research Funds for the Central Universities (No. 2242019R30001), and the EU H2020 RISE TESTBED2 project (No. 872172).

## REFERENCES

- [1] Y. Zeng, R. Zhang, J. L. Teng, "Wireless communications with unmanned aerial vehicles: opportunities and challenges," *IEEE Commun. Mag.*, vol. 54, no. 5, pp. 36–42, May 2016.
- [2] C.-X. Wang, J. Bian, J. Sun, W. Zhang, M. Zhang, "A survey of 5G channel measurements and models," *IEEE Commun. Surv. Tut.*, vol. 20, no. 4, pp. 3142–3168, Aug. 2018.
- [3] S. Wu, C.-X. Wang, H. Aggoune, M. M. Alwakeel, and X. You, "A general 3D non-stationary 5G wireless channel model," *IEEE Trans. Commun.*, vol. 66, no. 7, pp. 3065–3078, July 2018.
- [4] Z. Xiao, P. Xia, X. Xia, "Enabling UAV cellular with millimeter-wave communication: Potentials and approaches," *IEEE Commun. Mag.*, vol. 54, no. 5, pp. 66–73, May 2016.
- [5] R. Geise, A. Weiss, B. Neubauer, "Modulating features of field measurements with a UAV at millimeter wave frequencies," in *Proc. CAMA' 18*, Vasteras, Sweden, Nov. 2018, pp. 1–4.
- [6] H. Chang, J. Bian, C.-X. Wang, Z. Bai, W. Zhou, and H. Aggoune, "A 3D non-stationary wideband GBSM for low-altitude UAV-to-ground V2V MIMO channels," *IEEE Access*, vol. 7, no. 1, pp. 70719–70732, Dec. 2019.
- [7] Z. Khosravi, M. Gerasimenko, S. Andreev, and Y. Koucheryavy, "Performance evaluation of UAV-assisted mmWave operation in mobility-enabled urban deployments," in *Proc. TSP' 18*, Athens, Greece, Aug. 2018, pp. 1–5.
- [8] L. Kong, L. Ye, F. Wu, M. Tao, G. Chen, and A. V. Vasilakos, "Autonomous relay for millimeter-wave wireless communications," *IEEE J. Sel. Areas Commun.*, vol. 35, no. 9, pp. 2127–2136, Sep. 2017.
- [9] W. Zhong, L. Xu, Q. Zhu, X. Chen, J. Zhou, "MmWave beamforming for UAV communications with unstable beam pointing," *China Commun.*, vol. 16, no. 1, pp. 37–46, Feb. 2019.
- [10] W. Zhong, L. Xu, X. Liu, Q. Zhu, J. Zhou, "Adaptive beam design for UAV network with uniform plane array," *Physical Commun.*, vol. 34, no. 2019, pp. 58–65, Jun. 2019.
- [11] J. Zhao, F. Gao, L. Kuang, Q. Wu, and W. Jia, "Channel tracking with flight control system for UAV mmWave MIMO communications," *IEEE Commun. Lett.*, vol. 22, no. 6, pp. 1224–1227, Jun. 2018.
- [12] M. Gapeyenko, H. Y. I. Bor-Yaliniz, S. Andreev, and Y. Koucheryavy, "Effects of blockage in deploying mmWave drone base stations for beyond-5G networks," in *Proc. ICCW' 18*, Kansas City, USA, May 2018, pp. 1–6.
- [13] Q. Zhu, K. Jiang, X. Chen, W. Zhong, Y. Yang, "A Novel 3D Non-Stationary UAV-MIMO Channel Model and Its Statistical Properties," *China Commun.*, vol. 15, no. 12, pp. 147–158, Dec. 2018.
- [14] Q. Zhu, Y. Wang, K. Jiang, X. Chen, W. Zhong, N. Ahmed, "3D non-stationary geometry-based multi-input multi-output channel model for UAV-ground communication systems," *IET Microw., Antennas & Propag.*, vol. 8, no. 13, pp. 1104–1112, Apr. 2019.
- [15] W. Khawaja, O. Ozdemir, I. Guvenc, "UAV air-to-ground channel characterization for mmWave systems," in *Proc. VTC' 17*, Toronto, ON, Canada, Feb. 2017, pp. 1–5.
- [16] W. Khawaja, O. Ozdemir, I. Guvenc, "Temporal and spatial characteristics of mmWave propagation channels for UAVs," in *Proc. GSM' 18*, Boulder, CO, USA, May 2018, pp. 1–6.
- [17] Y. Miao, W. Fan, J. R. Piñero, Xuefeng Yin, Y. Gong, "Emulating UAV air-to-ground radio channel in multi-probe anechoic chamber," in *Proc. GC Wkshps' 18*, Abu Dhabi, United Arab Emirates, Dec. 2018, pp. 1–7.
- [18] Z. Cui, C. Briso, K. Guan, D. W. Matolak, C. Ramírez, B. Ai, et al., "Low-altitude UAV air-ground propagation channel measurement and analysis in a suburban environment at 3.9 GHz," *IET Microw., Antennas & Propag.*, vol. 13, no. 9, pp. 1503–1508, July 2019.
- [19] A. F. Molisch, F. Tufvesson, "Propagation channel models for next-generation wireless communications systems," *IEICE Trans. on Commun.*, vol. 97, no. 10, pp. 2022–2034, Oct. 2014.
- [20] M. Samimi, K. Wang, Y. Azar, G. N. Wong, R. Mayzus, H. Zhao, et al., "28 GHz angle of arrival and angle of departure analysis for outdoor cellular communications using steerable beam antennas in New York City," in *Proc. VTC' 13*, Dresden, Germany, June 2013, pp. 1–6.
- [21] J. Ko, Y. J. Cho, S. Hur, T. Kim, J. Park, A. F. Molisch, et al., "Millimeter-wave channel measurements and analysis for statistical spatial channel model in in-building and urban environments at 28 GHz," *IEEE Trans. on Wireless Commun.*, vol. 16, no. 9, pp. 5853–5868, Jun. 2017.
- [22] R. Sun, D. W. Matolak, "Over-harbor channel modeling with directional ground station antennas for the air-ground channel," in *Proc. MCC' 14*, Baltimore, MD, USA, Oct. 2014, pp. 382–387.